# Resonant Kα Spectroscopy of Solid-Density Aluminum Plasmas

B. I. Cho *et al.*

Phys. Rev. Lett. **109**, 245003 — Published 10 December 2012

DOI: 10.1103/PhysRevLett.109.245003

# Resonant K-alpha Spectroscopy of Solid Density Aluminum Plasmas

B. I. Cho[1*], K. Engelhorn[1], S. M. Vinko[2], H. -K. Chung[3], O. Ciricosta[2], D. S. Rackstraw[2], R. W. Falcone[1,4], C. R. D. Brown[5], T. Burian[6], J. Chalupský[6], C. Graves[7], V. Hájková[6], A. Higginbotham[2], L. Juha[6], J. Krzywinski[7], H. J. Lee[7], M. Messersmidt[7], C. Murphy[2], Y. Ping[8], N. Rohringer[9], A. Scherz[7], W. Schlotter[7], S. Toleikis[10], J. J. Turner[7], L. Vysin[6], T. Wang[7], B. Wu[7], U. Zastrau[11], D. Zhu[7], R. W. Lee[7], B. Nagler[7], J. S. Wark[2], and P. A. Heimann[7]

[1]*Lawrence Berkeley National Laboratory, 1 Cyclotron Road, CA 94720, USA*

[2]*Department of Physics, Clarendon Laboratory, University of Oxford, Parks Road, Oxford OX1 3PU, UK*

[3]*Atomic and Molecular Data Unit, Nuclear Data Section, IAEA, P.O. Box 100, A-1400, Vienna, Austria*

[4]*Department of Physics, University of California, Berkeley, California 94720, USA*

[5]*Plasma Physics Department, AWE Aldermaston, Reading, UK*

[6]*Institute of Physics ASCR, Na Slovance 2, 18221 Prague 8, Czech Republic*

[7]*SLAC National Accelerator Laboratory, 2575 Sand Hill Road, Menlo Park, CA 94025, USA*

[8]*Lawrence Livermore National Laboratory, 7000 East Avenue, Livermore, CA 94550, USA*

[9]*Max Planck Advanced Study Group, Center for Free-Electron Laser Science, DESY, Notkestraße 85, 22607 Hamburg, Germany*

[10]*Deutsches-Elektronensynchrotron DESY, Notkestrasse 85, 22603 Hamburg, Germany*

[11]*Institut für Optik und Quantenelektronik, Friedrich-Schiller-Universität, Max-Wien-Platz 1, 07743 Jena, Germany*

* Present Address: Department of Physics and Photon Science, Gwangju Institute of Science and Technology, Gwangju, 500-712, Korea

bicho@gist.ac.kr

**Abstract**

The X-ray intensities made available by X-ray free electron lasers (FEL) open up new X-ray – matter interaction channels not accessible with previous sources. We report here on the resonant generation of Kα emission, that is to say the production of copious Kα radiation by tuning the X-ray FEL pulse to photon energies *below* that of the K-edge of a solid aluminum sample. The sequential absorption of multiple photons in the same atom during the 80 fs pulse, with photons creating L-shell holes and then one resonantly exciting a K-shell electron into one of these holes, opens up a channel for the Kα production, as well as the absorption of further photons. We demonstrate rich spectra of such channels, and investigate the emission produced by tuning the FEL energy to the K-L transitions of those highly charged ions that have transition energies below the K-edge of the cold material. The spectra are sensitive to X-ray intensity dependent opacity effects, with ions containing L-shell holes readily reabsorbing the Kα radiation.

The recent development of the Linac Coherent Light Source (LCLS) has made it possible to generate for the first time extremely intense pulses of X-ray radiation: a typical pulse contains over $10^{12}$ X-ray photons within less than 80 fs [1]. With a typical bandwidth of less than 0.5 %, the resultant source represents an increase of nine orders of magnitude in peak spectral brightness compared to synchrotron light sources. The focused output from LCLS has already exceeded $10^{17}$ W/cm$^2$, a regime that opens up new possibilities in various fields of science, such as nanocrystallography [2], femtochemistry [3], and the study of matter in extreme conditions [4, 5].

Due to the high intensity that can be generated, multiphoton and nonlinear effects involving core states in atoms, molecules and solids are becoming increasingly important in the understanding of X-ray - matter interactions [5-9]. In particular, as we report in this letter, the sequential absorption of multiple photons can occur via channels which have been largely inaccessible to previous X-ray sources. When an element is irradiated by monochromatic radiation from a conventional X-ray source, Kα radiation can only be produced when the photon energy of the source exceeds the K-edge of the material, resulting in photo-ejection of a K-shell electron into the continuum, and the resultant filling of this hole by an L-shell electron via radiative decay. In contrast, as we show below, with the X-ray intensities available at LCLS, copious Kα radiation can be produced by irradiating a sample at photon energies well below the K-edge. For example, when the LCLS photon energy is tuned to the Kα energy, the source is so intense that during the pulse one X-ray photon can create an L-shell hole in a particular atom via photoionization (PI), which then opens up the resonant channel for a second photon to pump a

K-shell electron into the L-shell hole in the same atom - leading to an excited state that can now itself decay via the emission of Kα radiation.

Recently, resonant inner-shell transitions have been considered as essential processes to improve the current opacity and radiation transport models for high energy density (HED) matter such as astrophysical and fusion plasmas [10-12]. Although physical pictures of such systems mostly rely on various models, relevant atomic processes and plasma properties must be measured in benchmark experiments. Along with a demonstrated capability to create well-defined HED matter by isochoric heating of a solid with an intense X-ray pulse [5], the new X-ray - matter interaction channel opened by LCLS can provide a unique experimental means to investigate resonant processes. It is only one of many possibilities and in this letter we report on the observation of a rich array of Kα emission by irradiating an aluminum (Al) sample *below* the K-edge, which has a similar magnitude to the Kα emission above the K-edge. This result is surprising from the perspective of the traditional X-ray - matter interaction, but can be achieved via the inner-shell resonant processes driven by an intense X-ray pulse on a femtosecond timescale. The Kα emission is broadened by opacity effects caused by the X-ray absorption channel opened by the intensity of the focused X-ray pulse. The broadening is successfully described by numerical simulations.

The experiment was performed on the Soft X-Ray material science (SXR) instrument [13] at the LCLS. Quasi-monochromatic (0.5 % bandwidth) X-ray pulses in the photon energy range 1480 ~ 1580 eV, chosen below and slight above the K-edge of ground state Al, were incident on a 1 μm thick Al foil at an angle of 45 degrees. The LCLS pulse duration was estimated to be less than 80 fs, with each pulse typically containing $1.6 \times 10^{12}$ photons. The pulse

was focused to a 3 μm diameter spot on target, with a corresponding peak intensity in excess of $10^{17}$ W/cm$^2$. The principal diagnostic was X-ray emission spectroscopy, recorded with a flat Ammonium Dihydrogen Phosphate (101) crystal and an in-vacuum X-ray CCD. Further details on the setup can be found in the Ref. [5].

Above the K-edge, non-resonant Kα emission from a series of ionization states of Al has been recently reported [5]. In this separate paper, the pertinent processes of creating a hot - solid density plasma via direct K-shell PI with an intense LCLS pulse were discussed and the importance of electron-ion collisions was illustrated. It was also estimated that the temperature over 100 eV was achieved using simulations with a radiative-collisional code.

Below the absorption edge, because the X-ray photon energies are not sufficiently high to directly excite the Al K-shell in the single-photon regime, the *1s* states cannot be ionized directly and no Kα emission is in principle expected. The main interaction channel at these wavelengths is thus L-shell PI, which can absorb about 10 % of the pulse energy [14]. Although this fraction is relatively small, the X-ray pulse is sufficiently intense so that a large number of L-shell states in the system can still be ionized, indeed given the atomic and photon densities, a simple estimation shows that ~ 25 % of the atoms within the focal volume will contain an L-shell hole. Once created, they are relatively long-lived with a lifetime of 40 fs, determined by Auger decay from the valence band [15] and comparable with the duration of the X-ray pulse. Therefore, during the pulse itself, a strong new absorption channel in the ionized Al is created for X-rays precisely tuned to a specific inner-core transition: the LCLS photons can resonantly pump electrons from the full K-shell to the now-vacant L-shell.

These transitions have a much larger cross section than L-shell PI, so that as soon as the channel is created, resonant processes take over the X-ray - matter interaction dynamics. Since the K-shell hole life-time is short, on the order of a few fs [16], the resonant process gives rise to Kα emission at the resonance wavelength. Importantly, this emission is a unique signature of the resonance process since the energy required to directly photoionize a K-shell electron will always be larger than that required for K-L transition. This process is illustrated in Fig. 1a, where we plot the experimentally measured Kα emission in the spectral range 1470 ~ 1590 eV for a range of FEL excitation energies between 1480 eV and 1580 eV. Separately from the directly photoionized K-vacancy via above edge pumping, the resonant pumping of core states is clearly observed in the case where the X-ray photon energy matches the energy of a specific Kα transition.

We note that by scanning the X-ray photon energy, several different resonance channels are experimentally observed at increasingly higher emission energies. We identify the lowest-energy emission peak at 1487 eV as that arising from Al atoms with a single L-shell hole, i.e., the normal Kα emission as seen in cold samples, and the peaks at higher energies with atoms containing an increasing number of L-shell holes. Since the M-shell is delocalized in solid-density Al, these peaks correspond to Kα emission from higher charge states. Following the reference [17], we label the charge states according to their L-shell population in the final state, starting with the main Kα corresponding to IV (three delocalized M states and one L-shell hole after recombination).

Resonant emission from all possible charge states is observed up to X ($K^2L^1$). Albeit weak, the presence of this peak indicates that a state of very high ionization can be achieved even

in the case of below edge excitation. The reason for this lies in the efficient opening mechanisms for resonance channels in a hot dense system, combined with a strong coupling between X-rays and resonant inner-shell transitions once the relevant channels are present. It is important to note that for a resonance channel to be observed experimentally, the appropriate charge state must first and foremost be created by some alternative mechanism. Several processes compete in this regard, depending on the conditions present within the system and on the resonance charge state.

Emission from the lowest charge state IV is produced by a single L-shell PI, followed by a photo-induced K-L transition on the same ion. The radiative decay of this system produces the main Kα feature presented in Fig. 1. We note that the radiative yield from the L-shell is less than 4 % in Al (for IV) [18], and the majority of recombination thus proceeds via Auger decay. Whilst this process fills the K-shell hole, it produces an additional L-shell hole in the final state compared to radiative recombination. So while a sequence of radiative decay and resonance absorption cycles between two states of equal ionization, Auger decay increases the charge state of the ion by one and leads to the production of states which can no longer be resonantly pumped. These two competing processes are illustrated in Fig. 1b.

The Kα emission peaks originating from higher charge states will require several L-shell electrons to be ionized for the resonance channel to open. Only once the channel is made available can an X-ray photon drive the K-L transition, which will produce the observed Kα peaks by radiative decay. Experimentally we observe that the emission from higher charge states becomes weaker as the number of required L-shell holes is increased. To estimate this effect we plot in Fig. 1c the peak emission intensities as a function of charge state, alongside the number of X-ray photons (γ) required to photoionize the L-shell to that charge state. The observed

exponential trend is fully consistent with a sequential multi-photon ionization process of the L-shell being responsible for opening the various resonance channels.

An additional process that needs to be considered is electron collisional ionization of the L-shell. The L-shell in ground-state Al is bound by 73 eV [19] and both the electrons produced by L-shell PI as well as those produced by Auger decay are sufficiently energetic to collisionally ionize these states. Further, as these hot electrons proceed in thermalizing with the electrons in the system, the latter are heated. Once the temperature of the electrons in the continuum exceeds 10 ~ 20 eV, thermal ionization of the L-shell may take place.

These interlinked processes of initial L-shell PI, resonant K-L shell pumping, radiative and Auger decays, heating of the electrons in the conduction band and subsequent thermal L-shell ionization clearly lead to complex atomic kinetics throughout the pulse. Thus for more quantitative study, we model these resonant interactions using the collisional-radiative population kinetics code SCFLY [20]. It solves rate equations including photo-absorption, spontaneous and stimulated emissions, collisional excitation, ionization and recombination, thus providing atomic level populations, charge state distributions (CSD), electron density, temperature, photo-absorption and emission spectra as a function of time. SCFLY can include the effects of opacity via an escape factor formalism, but use of this shows little effect of the re-radiated emission on the atomic populations, as these are driven so strongly by the LCLS pulse. That is not, however, to say that opacity effects are not present: the re-radiated emission is indeed absorbed as it exits the plasma (e.g. Kα emission will be heavily absorbed by atoms containing a single L-shell hole), and thus the spectra indeed show opacity influences, even though the populations are only slightly perturbed by the atomic emission. As the atomic

radiation has little effect on atomic populations, we can make a good approximation to the opacity effects by taking into account the full experimental geometry. To do this we have discretized the target interaction region into a three-dimensional grid of points as shown in Fig 2a, solved the rate equations for each cell depending upon the transmission of LCLS pulse by previous cells. The emitted spectra are then calculated using the radiative transfer equation along the line-of-sight from each cell to the spectrometer. The mesh was determined by imposing that the distance between nearest neighbors is comparable to, or smaller than, the optical depth at the resonant wavelength.

We show the calculated spectra together with the experimental data in Fig 2c. Good agreement between the experiments and the simulations can be seen, with the resonant phenomena clearly observable. It is noted that the effect of collisions can be observed: although the on-resonance emission is the most intense peak in the spectrum, several other peaks are observed alongside it. These peaks cannot be explained in terms of a direct resonance, since the small bandwidth of the X-ray pulse makes direct K-shell photoexcitation of their corresponding charge states energetically forbidden. However, if electron-ion collisions can take place after an on-resonance K-shell photo-absorption but before the recombination, Kα emission from non-resonant charge states can be observed. Although this is a higher order many-body interaction process with a relatively weak cross section, it is observable and gives rise to the relatively wide resonance envelope in Fig. 2c.

Although collisional processes rely on sequential multi-photon absorption to initially seed energy to the system and open the resonance channels, once the resonance process is initiated, strong Auger recombination of the excited K-state will lead to very efficient heating. We note

that the absorption of the LCLS pulse and hence the electron temperatures predicted by SCFLY are comparable to those produced when pumping above the cold K-edge, where the initial cross section (due to a direct K-shell PI) is an order of magnitude greater than the below K-edge value. This somewhat counterintuitive result is illustrated in Fig. 2b. The relative CSD at peak X-ray intensity integrated over the duration of the pulse are also presented in Fig. 2d. We note that they produce quite different emission spectra in spite of the fact that the CSD for the various X-ray photon energies are similar, again this is primarily due to electron-ion collisions which efficiently populate a range of charge states regardless of whether or not they are on-resonance. It shows that the LCLS X-ray pulse below the K-edge is not only an efficient pump via the new absorption channel, but also an effective probe for a specific ionization state of the system.

The resonant inner-shell processes driven by the LCLS X-ray pulse also have significant effects on the opacity, which can be seen in the widths of the Kα lines. It is found that the line-widths of resonantly pumped Kα peaks are broader than those off-resonance. This broadening is particularly obvious if one compares the emission from a system pumped below and above the K-edge, for example at 1487 eV and 1580 eV. The experimental linewidths are determined by a Voigt profile; for an X-ray excitation at 1580 eV the non-resonant Kα peak is well-fitted by a Gaussian width of 1.3 eV and a Lorentzian width of 0.7 eV. The Gaussian width corresponds to the detector response function and the Lorentzian width agrees well with that determined from published data for the unresolved $K\alpha_{1,2}$ emission peak [21]. In the case of resonant excitation, the line is broadened in an intensity-dependent way: maintaining the same Gaussian width in the Voigt profile, we find a best-fit Lorenzian width of 1.9 eV at a peak intensity of $7 \times 10^{16}$ W/cm$^2$, and of 2.4 eV at $1 \times 10^{17}$ W/cm$^2$. These results are shown in Fig. 3a.

The Kα line shapes obtained by SCFLY calculation are also shown in Fig. 3b, alongside those calculated in the absence of opacity effects. Opacity broadens the line as the Kα of the IV charge state, for example, can be efficiently re-absorbed by atoms containing single L-shell holes: a situation more likely for below-edge pumping. Without accounting for optical depth effects, the resonant line width is similar to that in the non-resonant pumping case. Whereas when the optical depth is taken into account, the emission lines show the better agreement with experimental data. This phenomena is linked to the population of the resonant charge state, labeled as $R_{IV}$ in Fig 2d. Although it is quickly depleted to a higher charge state due to the faster Auger rate, simulation shows that the resonant state has a dominant population fraction in a certain time window (inset of Fig 2d). In addition, with the fact that the Kα emitting species ($K^1L^8$) is a product of photoexcitation of the absorbing species ($K^2L^7$), opacity is enhanced because of the strong emission. In contrast, no significant opacity broadening is observed for the non-resonant case, because the $K^2L^7$ is mainly created by a low probability spontaneous emission of $K^1L^8$, and its fractional population is low during the entire interaction period. We calculate an optical depth of around 200 nm within the interaction region of the main resonant Kα of Al IV, so that the 1 μm sample, which would be optically thin in the regime of a linear X-ray - matter interaction [14], is indeed optically thick at this wavelength. Given that our experimentally observed line-widths are slightly broader than those calculated using SCFLY including opacity effects, it is interesting to speculate whether other non-linear effects, such as Rabi flopping may be contributing to the line-width [7, 9]. However, a conclusive demonstration of such effects would need to employ targets sufficiently thin to avoid these opacity effects.

In summary, we have presented a detailed account of the physical processes pertaining to Al excited by intense X-ray radiation at photon energies below the K-edge. Sequential multi-photon absorption below the absorption edge is observed for a range of charge states, resonantly driving inner-shell transitions in the system on femtosecond timescales. We find if the X-ray pump is tuned to a below-edge resonance channel, similar X-ray absorption, Kα production and temperature can be reached in the system, compared with that found when pumping above the edge, despite the initial absorption cross sections differing by an order of magnitude in the ground-state. The LCLS X-ray pulse is also an effective probe of a specific charge state by producing resonant Kα emission in spite of the fact that efficient electron-ion collision rates determine the CSD. Further, a significant broadening of resonance emission peaks has been observed, which we attribute to opacity broadening. Due to the intensity dependent optical depth, the transparent sample at low intensity becomes optically thick with an intense LCLS X-ray pulse. These effects have implications for future studies of non-linear X-ray processes in dense samples.

Portions of this research were carried out on the SXR Instrument at the LCLS, a division of SLAC National Accelerator Laboratory and an Office of Science user facility operated by Stanford University for the U.S. Department of Energy. The SXR Instrument is funded by a consortium whose membership includes the LCLS, Stanford University through the Stanford Institute for Materials Energy Sciences (SIMES), Lawrence Berkeley National Laboratory (LBNL), University of Hamburg through the BMBF priority program FSP 301, and the Center for Free Electron Laser Science (CFEL). B.I.C., K.E., R.W.F. and P.A.H. acknowledge U.S. DOE Basic Energy Sciences, Contracts No. DE-AC03-76SF00098 and SSAA program Contract

No. DE-FG52-06NA26212. S.M.V., O.C. and J.S.W. thank the UK EPSRC for funding (EP/F020449/1 and EP/H035877/1). T.B., J.C., L.J. and L.V. appreciate funding by grants LA08024, ME10046, CZ.1.05/1.1.00/02.0061, CZ.1.07/2.3.00/483/20.0087, CZ.1.07/2.3.00/30.0057, P108/11/1312, P205/11/0571, P208/10/2302, and M100101221. U.Z. thanks the German Ministry for Education and Research (BMBF) for funding under FSP 301. C.D.M. was supported by UK EPSRC (EP/G007187/1).

**Reference**


[1] P. Emma *et al.*, Nature Photon. **4**, 641 (2010).

[2] H. N. Chapman *et al.*, Nature **470**, 73 (2011).

[3] K. J. Gaffney, and H. N. Chapman, Science **316**, 1444 (2007).

[4] B. Nagler *et al.*, Nature Physics **5**, 693 (2009).

[5] S. M. Vinko *et al.*, Nature **482**, 59 (2012).

[6] N. Rohringer, and R. Santra, Phys. Rev. A **76**, 033416 (2007).

[7] N. Rohringer, and R. Santra, Phys. Rev. A **77**, 053404 (2008).

[8] L. Young *et al.*, Nature **466**, 56 (2010).

[9] E. P. Kanter *et al.*, Phys. Rev. Lett. **107**, 233001 (2011).

[10] M. J. Seaton, and N. R. Badnell, Mon. Not. R. Astron. Soc. **354**, 457 (2004).

[11] J. E. Bailey *et al.*, Phys. Plasmas **16**, 058101 (2009).

[12] S. N. Nahar *et al.*, Phys. Rev. A **83**, 053417 (2011).

[13] P. Heimann *et al.*, Rev. Sci. Instrum. **82**, 093104 (2011).

[14] http://henke.lbl.gov/optical_constants/.

[15] C. O. Almbladh, A. L. Morales, and G. Grossmann, Phys. Rev. B **39**, 3489 (1989).

[16] P. Palmeri *et al.*, A&A **525** (2011).

[17] J. E. Bailey *et al.*, Laser Part. Beams **8**, 555 (1990).

[18] W. Bambynek *et al.*, Rev. Mod. Phys. **44**, 716 (1972).

[19] B. L. Henke, E. M. Gullikson, and J. C. Davis, Atomic Data Nucl. Data Tables **54**, 181 (1993).

[20] H. K. Chung, M. H. Chen, and R. W. Lee, High Energy Density Physics **3**, 57 (2007).

[21] M. O. Krause, and J. G. Ferreira, J. Phys. B **8**, 2007 (1975).

**Figures and Captions**

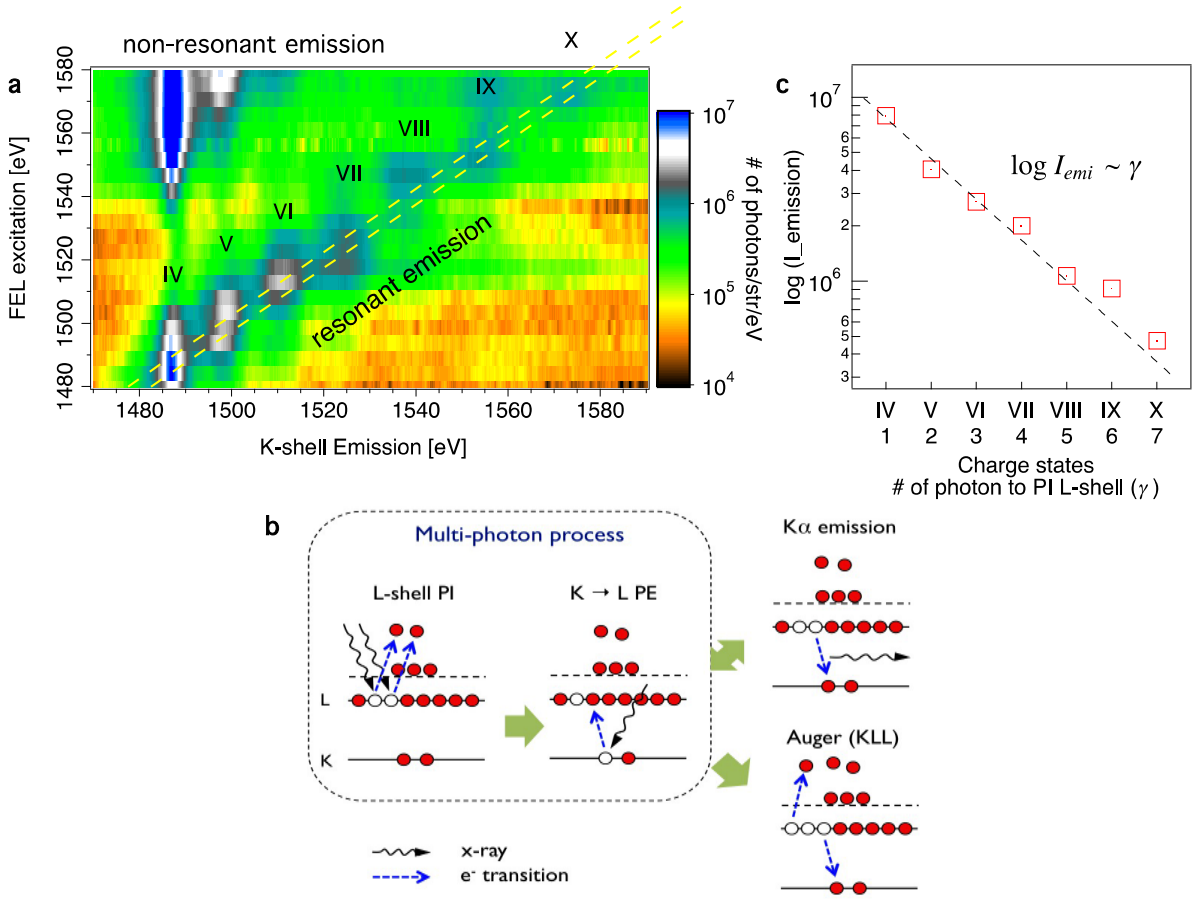


FIG 1. (a) K-shell emission spectra of solid density Al pumped with LCLS X-ray pulses at excitation energies ranging from 1480 ~ 1580 eV. Color code shows the emission intensity in a log scale. (b) The K-shell hole creation process when the X-ray photon energy is below the absorption edge. Preceding L-shell photoionizations (PI) are necessary for K-shell photoexcitation (PE). (c) Emission intensities from different charge states as a function of required number of vacancies in the L-shell. Each data point represents the strongest emission

from the most probable charge state on each resonance. Dotted line is an exponential fit. Intensity is presented in a log scale.

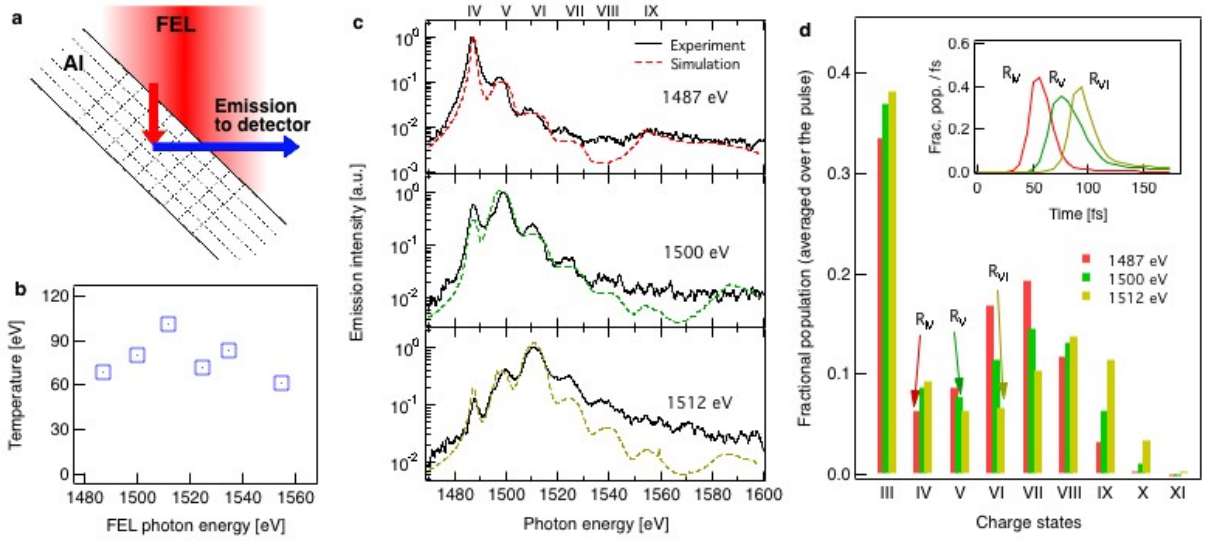


FIG. 2. (a) Geometrical consideration for SCFLY simulations. Each cell (100 nm × 100 nm × 100 nm) in the sample receives the X-ray flux based on the intensity profile of focal spot and transmission by preceding layers. Emission from each cell is reabsorbed by other cells in the line of sight to the detector. (b) Calculated electron temperatures at the end of X-ray pulse. (c) Calculated emission spectra (color dashed) at the first three resonances are compared with experiment (black solid). (d) Average CSD over the duration of X-ray pulse. (Inset) Temporal evolution of $R_{IV}$, $R_V$ and $R_{VI}$, which are resonant states with 1487 eV, 1500 eV and 1512 eV photon energies, respectively.

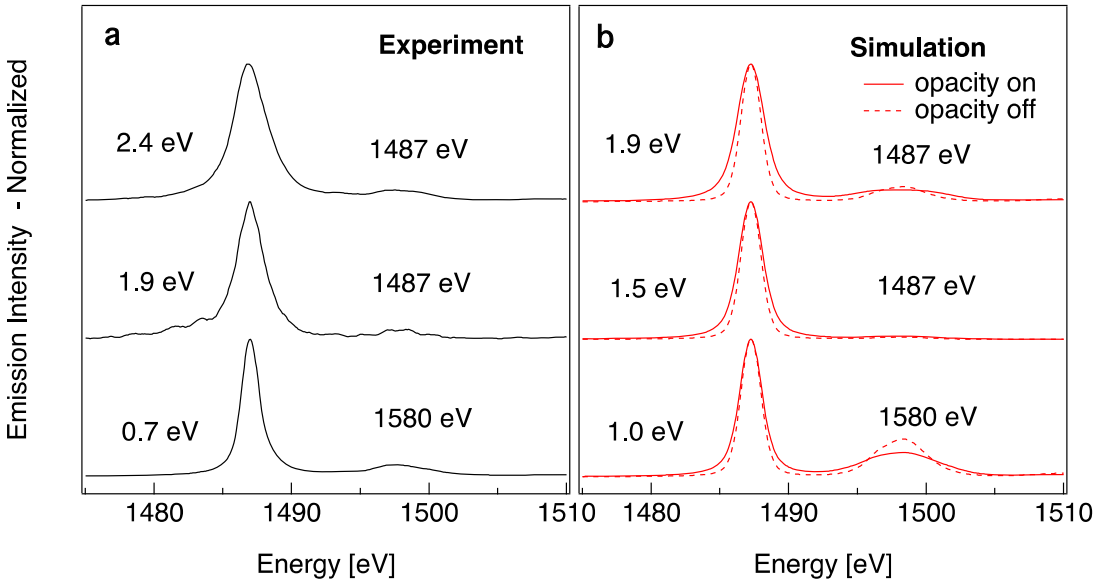


FIG. 3. (a) Experimental lineshapes of the main Kα emission for various FEL conditions. The bottom is for the non-resonant pumping (1580 eV), and the middle and top are for resonant pumping (1487 eV) with two different X-ray intensities, 0.7 and $1 \times 10^{17}$ W/cm$^2$, respectively. FWHM shown in the figure are determined by deconvolution of experimental broadening. (b) SCFLY simulation with equivalent conditions. For comparison, simulations with (solid lines) and without (dashed) opacity effects are displayed.